Redatuming of synthetic land data with shallow buried receivers using the virtual source method

Dmitry Alexandrov, Saint Petersburg State University; Andrey Bakulin and Roy Burnstad, EXPEC Advanced Research Center, Saudi Aramco*

Summary

We evaluate feasibility of virtual source redatuming with a synthetic 1D elastic dataset using receivers buried at 30 m. This work is to help validate an onshore field experiment in Saudi Arabia. In this study the receivers are located within the complex heterogeneous near surface. A major challenge is that our model contains a large number of highly contrasting layers and as a result is strongly contaminated with both surface and internal multiples. We demonstrate that virtual source redatuming is feasible under these conditions and delivers a reliable image of the target horizon. We examine various pre-processing options that can address multiples and improve virtual source imaging. The effects of source aperture and sampling are demonstrated on the final images. An optimal selection of the crosscorrelation time gate is made by observing the effects of different ghost arrivals on the resulting stacks. Using analysis of the correlation gathers, we quantify improvements introduced by up-down wavefield separation using land dual-sensor summation and justify the selection of a larger summation aperture.

Introduction

Onshore seismic monitoring is often conducted with shallow buried receivers to improve repeatability (Schissele et al., 2009). Depth of burial can vary from a few meters to tens of meters depending on near-surface complexity. The use of buried sensors gives an opportunity to perform virtual source redatuming to the receiver level without any knowledge of the velocity model above the receivers. It has been shown that redatuming can simplify the wavefield and eliminate distortions associated with heterogeneity located between the source and receivers (Bakulin and Calvert, 2006). In addition, redatuming is expected to improve survey repeatability and correct for diurnal and seasonal variations, small changes in acquisition geometry, as well as differences in shot coupling (Bakulin and Calvert, 2006). Previous work mainly focused on redatuming data acquired with deep receivers (a few hundred meters to kilometers below the surface). Recently Bakulin et al. (2012) reported usage of buried receivers at 30 to 50 m depth in a desert environment. In this study we analyze the shallow redatuming problem using a realistic synthetic model and focus on obtaining reliable images of the target horizon at 2 km depth.

Velocity model and acquisition geometry

Figure 1a shows an idealized 1D model derived from sonic log and check shot data acquired over an onshore field in Saudi Arabia. The model includes a free surface and an uppermost low-velocity layer comprised of 16 m of sand cover. Acquisition geometry is based on a recent field experiment over an onshore field in Saudi Arabia (Bakulin et al., 2012). Vertical geophones are buried below the sand layer at a depth of 30 m. Seismic data are generated using a vertical force source at the surface, simulating a surface vibrator. We use an inline source sampling of 7.5 m to simulate the actual field acquisition geometry. The presence of a large number of highly contrasting layers throughout the overburden leads to generation of a significant number of internal and surface multiples. This is confirmed by analysis of synthetic VSP data from the same model following the methodology reported by Lesnikov and Owusu (2011).

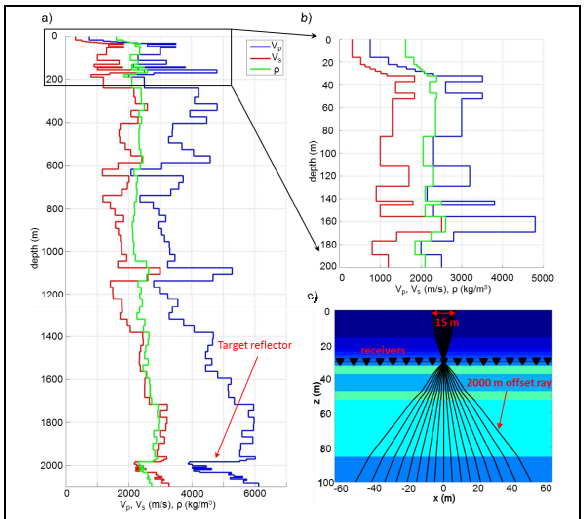

Figure 1: The subsurface model used for the feasibility study: (a) P- and S-wave velocities and densities from the surface to the target at 2 km, (b) a zoom of the near-surface portion, (c) ray paths for reflections from the target horizon with offsets of up to 2000 m. Note the strong ray bending and near-vertical propagation in the shallowest low-velocity sand layer.

The virtual source method is a redatuming technique that uses experimentally measured Green's functions from buried receivers and as such does not require knowledge of any velocity model (Bakulin and Calvert, 2006). Thus surface sources are redatumed from the surface to subsurface receiver locations. Such an approach is attractive for cases when the near-surface is complex. The method requires adequate source sampling in order for constructive and destructive interference to work.

DOI http://dx.doi.org/10.1190/segam2012-0295.1

Construction of virtual source gathers involves cross-correlation of the wavefields and summation over an aperture of surface sources. This technique is valid for a generally heterogeneous anisotropic medium of any complexity inside the area of integration. The assumption is made that the medium outside this integration area is homogeneous (Wapenaar et al., 2010). This implies, in particular, the absence of a free surface. For land applications with free-surface multiples, this poses a serious problem that remains to be addressed.

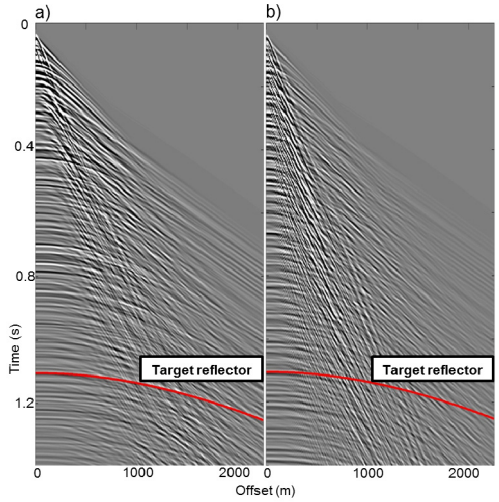

Figure 2: Common-shot gather for the 1D model shown in Figure 1: (a) without free surface, (b) with free surface.

Figure 2 shows synthetic seismograms for the 1D model with and without a free surface. The free surface leads to the generation of a large number of surface-related multiples as well as surface waves which significantly obscure primary reflections.

We test several different approaches to generate pre-stack virtual source data. Then we introduce NMO corrections into pre-stack virtual source data and sum, thus obtaining what we refer to as a 1D stack of virtual source data that represents a 1D image in this case. To evaluate these images, we compare them with a ground truth response image of data generated from actual sources at the receiver locations as well as a VSP corridor stack. 1D virtual source stacks are also compared to conventional stacks obtained without redatuming (static corrections only). Our goal is to devise a workflow and parameters that provide an optimum image of a target horizon at a depth of 2 km.

Redatuming with virtual source method

To generate virtual source data from the initial synthetic shot record we follow a simple workflow. First, we perform noise removal by filtering in the f-k domain to attenuate linear arrivals such as surface and refracted waves. Noise removal is followed by crosscorrelation and summation over an aperture of sources (Bakulin and Calvert, 2006). To produce a stacked image we apply an NMO correction and stack.

Effect of the aperture size

Virtual source theory requires stacking over a closed surface covered with sources. In practice, stacking is limited to some finite aperture, which includes a stationary phase point. Ray tracing results (Figure 1c) show that a surface aperture of only 15 m is enough to generate the range of required offsets on virtual source data for this model, target depth and acquisition configuration. Rapid increases in near-surface velocity with depth (Figure 1b) cause rays with shooting angles greater than 5^o to reach critical angle in one of the shallow layers and do not produce reflections from the target. Of course ray tracing is only a high-frequency approximation of the wave propagation, while in field datasets relatively low frequencies would tunnel through thin high-velocity layers. To account for these effects, we consider larger apertures than those predicted by ray tracing.

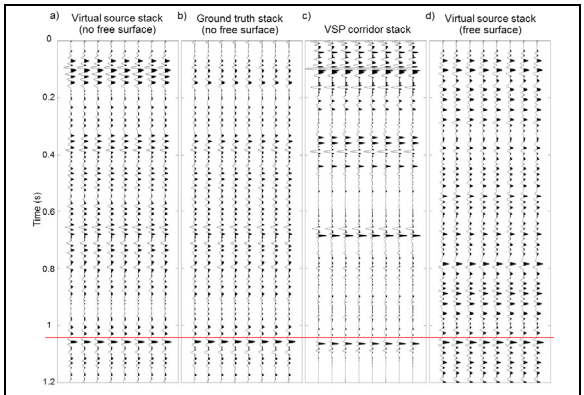

Figure 3: Comparison of 1D stacks including (a) a virtual source stack for the model without a free surface, (b) the ground truth stack for the model without a free surface obtained with actual buried sources at receiver locations, (c) a VSP corridor stack and (d) the virtual source stack for the model with a free surface. Observe additional events related to internal multiples on (a) and (b) that are not present on (c). Likewise observe additional events related to surface multiples that are present on (d) but not on (a).

Figure 3a shows a virtual source 1D stack for the model without a free surface. The amplitude level of the stack is normalized with respect to the target reflection shown by the red line. This stack is compared with a ground truth stack (Figure 3b), obtained using the same NMO correction and stacking. The ground truth response is re-computed with sources positioned at a 30 m depth. It assumes a homogeneous half-space above 30 m with the same properties as the source layer (Mehta et al., 2007). The

DOI http://dx.doi.org/10.1190/segam2012-0295.1

virtual source stack is almost identical to the ground truth (Figure 3a vs 3b). Figure 3c displays a VSP corridor stack that contains only primary reflections. While some arrivals on the ground truth stack match those from the VSP stack, most of them do not because of the presence of internal multiples. Strong free-surface multiples generate additional spurious events on the virtual source stack (Figure 3d). In all cases however, the target reflection (red line), is readily identifiable. Results from this study suggest that the best virtual source image is achieved with an aperture of 200 m - significantly larger than the 15 m predicted by ray theory**.**

Time gate selection

It is also found that extending the downgoing time gate to include several events after the direct arrival increases the amplitude of target reflection on the virtual source 1D stack. This is illustrated in Figure 4, where we compare virtual source stack sections computed with different time gates. The amplitude of the target reflection is highlighted with a red arrow. Red frames indicate parts of traces which changed with time gate variation. Increasing a gate length from 60 ms to 120 ms increases the amplitude of target reflection compared to background arrivals. Time gate lengths of more than 200 ms for the downgoing wavefield do not significantly change the picture.

The best estimates for the time gate (180 ms) and trace aperture (200 m) were used to build the virtual source 1D stack shown in the Figure 3.

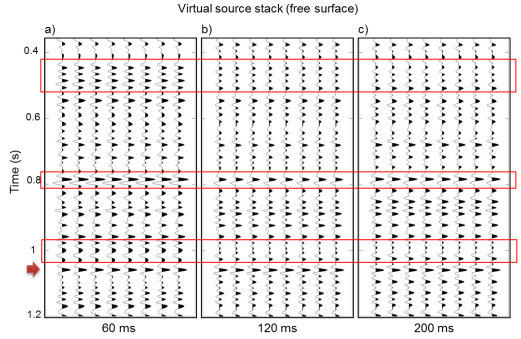

Figure 4: Virtual source 1D stacks obtained with a source aperture of 200 m and different time gate lengths including (a) 60 ms, (b) 120 ms and (c) 200 ms.

Why longer time gates may help

To illustrate why increasing the time gate length may be helpful, we examine this issue in more detail. Figure 5a shows the downgoing wave field after production preprocessing. In this case the downgoing wavefield was obtained by using hydrophone and geophone summation as described in the next section. Therefore we are confident that it indeed contains predominantly downgoing energy and is not contaminated by any upgoing events. Stronger events are identified by ray tracing as source-side ghost arrivals resulting from up-going shallow reflections. There are two types of receiver ghosts on the seismogram, shallow and deeper ghosts. The first type is generated mainly in the uppermost layers, above the sensor array. It is restricted in maximum offset because of small critical angles in subsurface layers. Generally the shallow ghost reflections have similar moveout to direct arrivals. A deeper ghost arises from horizons below the receivers, bounces back from the free surface and therefore is visible over a larger range of offsets with flatter moveout.

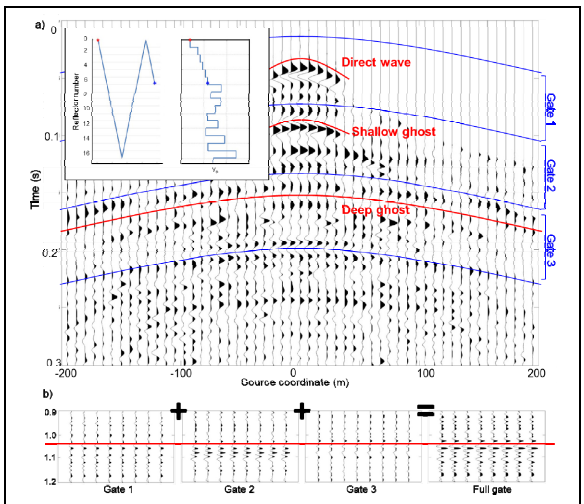

Figure 5: (a) The downgoing wavefield after production-type preprocessing (gain ~ $v_{nmo}(t)\bullet t$ is applied). Different time gates used for crosscorrelation are displayed. The inset shows origin of the deep ghosts that bounce off reflectors below the receivers and then return to the surface. (b) Zooms of virtual source 1D stacks after redatuming for each time gate. "Full gate" is comprised of a combination of gates 1, 2 and 3 shown on (a).

While we could have selected a short time gate leaving the direct wave only, we studied the contribution of these later ghost arrivals on virtual source gathers and 1D stacks. For this analysis it is instructive to consider the pre-stack correlation gather (Figure 6). This gather comprises crosscorrelations of the time windowed downgoing field, from Figure 5a, with the upgoing field before summation. Stacking of this gather yields a single virtual source trace for a particular offset. Analysis of the correlation gather shows that the direct wave and the shallow ghost events correlate with the upgoing field to produce strong steep events dominating near offsets. In contrast, deeper ghosts produce events which are much weaker and flatter, but distributed over a larger range of offsets. Selection of a larger trace aperture, on the order of 200 m, maximizes contributions from deep ghost reflections.

To evaluate the contribution of different arrivals to a target reflection, the original time gate used for crosscorrelation

DOI http://dx.doi.org/10.1190/segam2012-0295.1

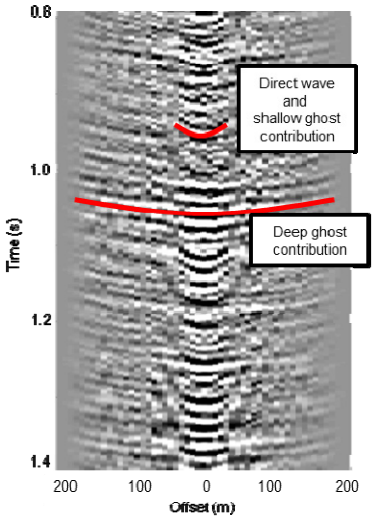

Figure 6: Pre-stack correlation gather before summation for a 200 m offset trace. There is a significant moveout difference between the contribution from direct arrival (and shallow ghosts) and deep ghosts.

was divided into three distinct gates: shallow (direct arrival only), medium (the shallow and deep ghost reflections), and deep (the deep ghost reflections only) (Figure 5a). While the shallow gate produces a virtual source 1D stack with a target reflection at the correct time, the amplitude level of this arrival is almost the same as that of background events (Figure 5b). Using the middle time gate approximately doubles the amplitude of the target reflection. It also introduces artefacts below the target reflection. A virtual source stack obtained using the deep time gate has lower amplitude at the target reflection, with lower levels of artefacts than observed with the middle gate. The best result is obtained when all three gates are combined into a single 180 ms gate. This suggests that direct arrival and source-related ghosts all contribute to the target reflection and improve the signal-to-noise ratio on the final virtual source image.

Wavefield separation using dual-sensor summation

To a certain degree the issue of surface multiples and spurious crosscorrelation events can be addressed by an approach suggested by Mehta et al. (2007): up-down wavefield separation before crosscorrelation. This approach allows us to remove spurious events generated by the horizons below the receiver line and also addresses multiples related to the free surface. Following best practice for land, geophone and hydrophone responses are computed and combined after noise removal to perform wavefield separation. Field datasets may use adaptive scaling prior to summation. The rest of the processing steps, including the virtual source creation, follow the workflow described earlier. Virtual source images with wavefield separation introduce additional improvements. Figure 7 illustrates a significant increase of signal-to-noise ratio in case of up-down wavefield decomposition prior to crosscorrelation.

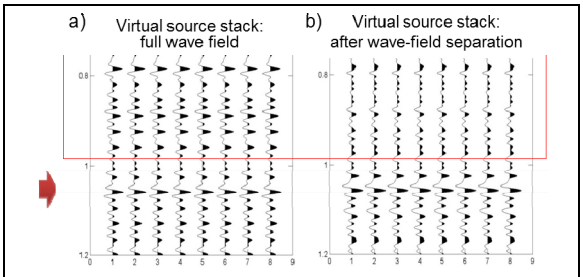

Figure 7: Zooms of virtual source 1D stacks after redatuming using (a) full wavefield and (b) decomposed wavefield. Note reduction in background reflectivity level above the target on (b) which makes it closer to the VSP corridor stack (Figure 3c) indicating that wavefield separation removes many multiples.

Conclusions

We have successfully demonstrated feasibility of redatuming land seismic data with shallow buried sensors at 30 m depth. Despite receivers being located in the highly heterogeneous near surface, redatuming produces a reliable image of the target reflector. Due to the presence of highly contrasting layers throughout the entire overburden, the synthetic data contains large number of internal and free-surface multiplies that create real and spurious events on the virtual source gather and stack. Large source aperture and longer time gate used for correlation enhances the target reflection compared to the background events, though they also increase the number of events in other parts of the section. Numerical tests suggest that for this model the best virtual source image is obtained with a source aperture of 200 m and gate length of 180 ms. Up-down wavefield separation using dual-sensor summation leads to an improved signal-to-noise ratio on the virtual source gather. When utilizing a longer time gate, we confirm that the improvements originate from an additional contribution to target reflections coming from crosscorrelation of downgoing source-related ghosts with the corresponding upgoing energy. Therefore, for an optimal image, source-side ghosts should be included in the time gate. In the future studies we will investigate whether inclusion of the source-side ghosts has any impact on the repeatability of the virtual source image.

Acknowledgements

We would like to thank Saudi Aramco for allowing us to publish this work.

DOI http://dx.doi.org/10.1190/segam2012-0295.1

http://dx.doi.org/10.1190/segam2012-0295.1

EDITED REFERENCES

Note: This reference list is a copy-edited version of the reference list submitted by the author. Reference lists for the 2012 SEG Technical Program Expanded Abstracts have been copy edited so that references provided with the online metadata for each paper will achieve a high degree of linking to cited sources that appear on the Web.

REFERENCES

Bakulin, A., and R. Calvert, 2006, The virtual source method: Theory and case study: Geophysics, **71**, no. 4, SI139–SI150.

Bakulin, A., M. Jervis, R. Burnstad, and P. Kelamis, 2012, The feasibility of permanent land seismic monitoring with buried geophones and hydrophones in a desert environment: 74th Annual International Conference and Exhibition, EAGE, Extended Abstracts, X039.

Lesnikov, V., and J. Owusu, 2011, Understanding the mechanism of interbed multiple generation using VSP data: 81st Annual International Meeting, SEG, Expanded Abstracts, 4258–4262.

Mehta, K., A. Bakulin, J. Sheiman, R. Calvert, and R. Snieder, 2007, Improving the virtual source method by wavefield separation: Geophysics, **72**, no. 6, V79–V86.

Schissele, E., E. Forgues, J. Echappé, J. Meunier, O. de Pellegars, and C. Hubans, 2009, Seismic repeatability — Is there a limit?: 71st Annual International Conference and Exhibition, EAGE, Extended Abstracts, V021.

Wapenaar, K., E. Slob, R. Snieder, and A. Curtis, 2010, Tutorial on seismic interferometry: Part 2 — Underlying theory and new advances: Geophysics, **75**, 75211–75227.